Proceedings of the ASME 2015 Dynamic Systems and Control Conference
DSCC2015
October 28-30, 2015, Columbus, Ohio, USA

DSCC2015-9813

DRAFT: COMPLETE DYNAMIC MODELLING OF FLEXIBLE JOINT ROBOTS

Yu Zhao
Dept. of Mechanical Engineering
University of California
Berkeley, California 94720
Email: yzhao334@berkeley.edu

Cong Wang
Dept. of Mechanical Engineering
University of California
Berkeley, California 94720
Email: wangcong@berkeley.edu

Xiaowen Yu
Dept. of Mechanical Engineering
University of California
Berkeley, California 94720
Email: aliceyu@berkeley.edu

Masayoshi Tomizuka
Dept. of Mechanical Engineering
University of California
Berkeley, California 94720
Email: tomizuka@me.berkeley.edu

ABSTRACT

Joint flexibility is common in industrial robots that have geared joints. In order to design a precision motion controller that compensates the effects of joint elasticity, an accurate dynamic model of flexible joint robots is required. The models that are commonly used ignore the gyroscopic interactions between the motors and links. In order to evaluate the influence of the ignored gyroscopic interaction, a complete dynamic model for flexible joint robots is derived in this paper. It is shown that when to realize high accuracy for high velocity trajectory tracking, the motor inertia is non-negligible compared to link inertia, and that the neglected interaction terms must be taken into account.

INTRODUCTION

Joint flexibility is common in robot manipulators. It is introduced by transmission components such as harmonic drives, transmission belts and long shafts [1]. For accurate trajectory tracking, the effects of transmission flexibility must be taken into account. Several control approaches are developed in order to achieve high accuracy trajectory tracking for flexible joint robot. These approaches include but not limited to the integrator backstepping [2], the dynamic surface control [3], the adaptive robust control [4], and the iterative learning control [5].

Typically, a reduced dynamic model [6, 7] is used for controller design. However, the reduced dynamic model is only an approximation under the assumption that the kinetic energy of the motor rotors is due mainly to their own axial rotation about the motor shafts. In human-robot interaction applications, robot mass is required to be very low in order to reduce the injury risk [8]. For robots with flexible joints, the reduction of link mass increases the gyroscopic interaction between the motors and the links, and invalidates the fundamental assumption of the reduced dynamic model. In particular, the gyroscopic interaction is non-negligible in high accuracy trajectory tracking for industrial robots moving at high velocities. The gyroscopic interaction corresponds to an motor acceleration related term that is not included in the common reduced dynamic models. This extra term changes the order of the model and affects model identification. A complete dynamic model that takes the gyroscopic interactions into account is desirable for compensating robot dynamics in precision control.

In this paper, the complete dynamic model of flexible joint robots is derived using Lagrangian Dynamics. Based on the dynamic model, the influence of the gyroscopic interaction can be evaluated. A precision trajectory tracking simulation is used to demonstrate the influence.

DYNAMIC MODELLING

Because of the flexibility in the gear transmission, the rotors of the motors are not connected to the links rigidly, and thus become individual bodies in the system. Their kinetic energy and potential energy have to be counted separately from those of the links.

Kinetic and Potential Energy of the Motors and Links

Let $q_\ell = [q_{\ell 1}, q_{\ell 2}, \cdots, q_{\ell n}] \in \mathbb{R}^n$ be the vector of rotation angles of the links, $q_m = [q_{m1}, q_{m2}, \cdots, q_{mn}] \in \mathbb{R}^n$ be the vector of rotation angles of the motor rotors. The total *kinetic energy* T_ℓ and total *gravitational potential energy* U_ℓ of the links are

$$T_\ell = \frac{1}{2}\dot{q_\ell}^T M(q_\ell)\dot{q}_\ell \tag{1a}$$

$$U_\ell = U_\ell(q_\ell) \tag{1b}$$

whereas the *kinetic energy* T_{mi} and *gravitational potential energy* U_{mi} of the rotor of the i-th motor are

$$T_{mi} = \frac{1}{2}\begin{bmatrix} \dot{p_{mi}} \\ \omega_{mi} \end{bmatrix}^T \begin{bmatrix} m_{mi}I & 0 \\ 0 & I_{mi} \end{bmatrix} \begin{bmatrix} \dot{p_{mi}} \\ \omega_{mi} \end{bmatrix} \tag{2a}$$

$$U_{mi} = -m_{mi}\, g^T\, p_{mi} \tag{2b}$$

where p_{mi} is the position of the center of gravity, ω_{mi} is the angular velocity, m_{mi} is the mass, I_{mi} is the moment of inertia, g is the gravitational acceleration. Assuming that the inertia of the motor rotor is symmetric about its rotation axis, its center of gravity and the velocity twist [9] are given by the forward kinematics and differential kinematics

$$p_{mi} = p_{mi}(q_\ell) \tag{3a}$$

$$\begin{bmatrix} \dot{p_{mi}} \\ \omega_{mi} \end{bmatrix} = J_{\ell i}(q_\ell)\dot{q}_\ell + \begin{bmatrix} 0 \\ n_{mi}(q_\ell) \end{bmatrix}\dot{q}_{mi} \tag{3b}$$

where $J_{\ell i}$ is the Jacobian of the transformation from the robot base frame (the inertia frame) to the motor installation frame (aligned with $q_{mi} = 0$). n_{mi} is the unit direction vector of the motor rotation axis in the inertia frame. The moment of inertia of the i-th motor expressed in the inertia frame is

$$\begin{aligned} I_{mi} &= R_{mi\ell}(q_\ell)R_{mim}(q_{mi})I^b_{mi}R^T_{mim}(q_{mi})R^T_{mi\ell}(q_\ell) \\ &= R_{mi\ell}(q_\ell)I^b_{mi}R^T_{mi\ell}(q_\ell) \end{aligned} \tag{4}$$

where I^b_{mi} is the inertia of the rotor in its corotational frame (the rotor frame), which is a constant. The $R_{mi\ell}(q_\ell)$ denotes the rotation from the inertia frame to the motor installation frame, and $R_{mim}(q_{mi})$ denotes the rotation from the motor install frame to the rotor frame.

Based on Eqn. (2a), (2b), (3a), (3b), and (4), the motor kinetic energy and gravitational energy of the motor rotors are

$$\begin{aligned} T_{mi} = &\frac{1}{2}\dot{q}^T_\ell J^T_{\ell i}(q_\ell)\begin{bmatrix} m_{mi}I & 0 \\ 0 & I_{mi}(q_\ell) \end{bmatrix} J_{\ell i}(q_\ell)\dot{q}_\ell + \\ &\dot{q}_{mi}\begin{bmatrix} 0 & n^T_{mi}(q_\ell)I_{mi}(q_\ell) \end{bmatrix} J_{\ell i}(q_\ell)\dot{q}_\ell + \\ &\frac{1}{2}\dot{q}_{mi}n^T_{mi}(q_\ell)I_{mi}(q_\ell)n_{mi}(q_\ell)\dot{q}_{mi} \end{aligned} \tag{5a}$$

$$U_{mi} = -m_{mi}g^T p_{mi}(q_\ell) \tag{5b}$$

Based on Eqn. (1a), and (5a), the total kinetic energy of the system is

$$\begin{aligned} T &= T_\ell + \textstyle\sum_{i=1}^n T_{mi} \\ &= \frac{1}{2}\dot{q}^T_\ell M_\ell(q_\ell)\dot{q}_\ell + \frac{1}{2}\dot{q}^T_m M_m \dot{q}_m + \dot{q}^T_\ell M_{m\ell}(q_\ell)\dot{q}_m \end{aligned} \tag{6}$$

in which,

$$M_\ell(q_\ell) = M(q_\ell) + \sum_{i=1}^n J^T_{\ell i}(q_\ell)\begin{bmatrix} m_{mi}I & 0 \\ 0 & I_{mi}(q_\ell) \end{bmatrix} J_{\ell i}(q_\ell)$$

is the lumped link inertia matrix, which is also called a 'load side inertia matrix' in [Wenjie, dualstage ILC]. The motor side inertia matrix

$$M_m = \mathrm{diag}(\sum_{i=1}^n n^T_{mi}R_{mi\ell}I^b_{mi}R^T_{mi\ell}n_{mi}) = \mathrm{diag}(\sum_{i=1}^n [0,0,1]I^b_{mi}[0,0,1]^T)$$

is an constant diagonal matrix. The coupled energy term involves both motor rotor velocity and link velocity, and reflects the gyroscopic interaction between (the rotors of) the motors and the links

$$\dot{q}^T_\ell M_{m\ell}(q_\ell)\dot{q}_m = \dot{q}^T_\ell \begin{bmatrix} 0 & s_{1,2}(q_\ell) & \cdots & s_{1,n}(q_\ell) \\ 0 & 0 & \cdots & s_{2,n}(q_\ell) \\ \vdots & \vdots & \ddots & \vdots \\ 0 & 0 & \cdots & s_{n-1,n}(q_\ell) \\ 0 & 0 & \cdot & 0 \end{bmatrix} \dot{q}_m \tag{7}$$

where $s_{i,j}(q_\ell) = \alpha(q_\ell, j)\, n^T_{mj}(q_\ell)n_{\ell i}(q_\ell)$. $\alpha(q_\ell, j)$ is the I_{zz} term of $I_{mj}(q_\ell)$, $n_{mj}(q_\ell)$ is the unit direction vector of the rotation axis of the j-th motor, and $n_{\ell i}(q_\ell)$ is the unit direction vector of the

rotation axis of the $i-th$ link. Note that $s_{i,j}=0$ if $i \geq j$, because usually the installation frame of the j-th motor is only determined by joint 1 to $j-1$.

The total potential energy of the system is

$$\begin{aligned} U &= U_\ell + \textstyle\sum_{i=1}^{n} U_{mi} + U_e \\ &= U_{m\ell}(q_\ell) + \frac{1}{2}(N^{-1}q_m - q_\ell)^T K_J (N^{-1}q_m - q_\ell) \end{aligned} \tag{8}$$

where $U_{m\ell}$ represents the total gravitational potential energy of the motors and links. N is the transmission gear ratio, K_J and D_J are the joint stiffness and damping, and U_e is the elasticity energy. It is assumed that the joint elasticity is linear. In addition, if the transmission error $\tilde{q}(q_m)$ is taken into account [5], the elasticity energy can be modified as

$$U_e = \frac{1}{2}(N^{-1}q_m - q_\ell - \tilde{q}(q_m))^T K_J (N^{-1}q_m - q_\ell - \tilde{q}(q_m))$$

Lagrange's Equations of Motion

The Lagrangian is given by $L = T - U$, where the kinetic energy T is given by Eqn. (6), and the potential energy U is given by Eqn. (8). Following the Lagrangian approach, the equations of motion of a flexible joint robot are given by

$$\frac{\mathrm{d}}{\mathrm{d}t}\left(\frac{\partial L}{\partial \dot{q}_\ell}\right) - \frac{\partial L}{\partial q_\ell} = Q_\ell \tag{9a}$$

$$\frac{\mathrm{d}}{\mathrm{d}t}\left(\frac{\partial L}{\partial \dot{q}_m}\right) - \frac{\partial L}{\partial q_m} = Q_m \tag{9b}$$

where Q_ℓ and Q_m are the non-conservative generalized force performing work on the dimensions q_ℓ and q_m. Evaluating the derivatives in Eqn. (9a) and (9b) leads to a set of nonlinear differential equations. This set of nonlinear differential equations is called the *complete dynamic model*

$$\begin{aligned} &M_\ell(q_\ell)\ddot{q}_\ell + M_{m\ell}(q_\ell)\ddot{q}_m + C(q_\ell,\dot{q}_\ell)\dot{q}_\ell + C_1(q_\ell,\dot{q}_\ell)\dot{q}_m + g(q_\ell) \\ &\quad = K_J(N^{-1}q_m - q_\ell) + D_J(N^{-1}\dot{q}_m - \dot{q}_\ell) + d_\ell \qquad (10a) \\ &M_m\ddot{q}_m + M_{m\ell}^T(q_\ell)\ddot{q}_\ell + C_2(q_\ell,\dot{q}_\ell)\dot{q}_\ell = \tau_m + d_m \\ &\quad -N^{-1}\left[K_J(N^{-1}q_m - q_\ell) + D_J(N^{-1}\dot{q}_m - \dot{q}_\ell)\right] \qquad (10b) \end{aligned}$$

where $C(q_\ell,\dot{q}_\ell)\dot{q}_\ell$, $C_1(q_\ell,\dot{q}_\ell)\dot{q}_m$, and $C_2(q_\ell,\dot{q}_\ell)\dot{q}_\ell$ correspond to Coriolis and centrifugal force, $g(q_\ell)$ is the gravity term, and d_ℓ and d_m are load side and motor side state-dependent disturbances caused by transmission error, friction, etc.

The Coriolis and centrifugal force terms can be written as $V[\dot{q}_\ell,\dot{q}_m]^T$, where the V matrix can be expressed as

$$V = \begin{bmatrix} C(q_\ell,\dot{q}_\ell) & C_1(q_\ell,\dot{q}_\ell) \\ C_2(q_\ell,\dot{q}_\ell) & 0 \end{bmatrix}$$

with

$$\begin{aligned} C(q_\ell,\dot{q}_\ell) &= \frac{1}{2}\sum_k \left(\frac{\partial M_{\ell(i,j)}}{\partial q_{\ell(k)}} + \frac{\partial M_{\ell(i,k)}}{\partial q_{\ell(j)}} - \frac{\partial M_{\ell(j,k)}}{\partial q_{\ell(i)}}\right)\dot{q}_{\ell(k)} \\ C_1(q_\ell,\dot{q}_\ell) &= \sum_k \left(\frac{\partial M_{m\ell(i,j)}}{\partial q_{\ell(k)}} - \frac{\partial M_{m\ell(j,k)}^T}{\partial q_{\ell(i)}}\right)\dot{q}_{\ell(k)} \\ C_2(q_\ell,\dot{q}_\ell) &= \sum_k \left(\frac{\partial M_{m\ell(i,j)}^T}{\partial q_{\ell(k)}}\right)\dot{q}_{\ell(k)} \end{aligned}$$

Compared to the reduced model [6]

$$\begin{aligned} &M_\ell(q_\ell)\ddot{q}_\ell + C(q_\ell,\dot{q}_\ell)\dot{q}_\ell + g(q_\ell) \\ &\quad = K_J(N^{-1}q_m - q_\ell) + D_J(N^{-1}\dot{q}_m - \dot{q}_\ell) + d_\ell \qquad (11a) \\ &M_m\ddot{q}_m = \tau_m + d_m \\ &\quad -N^{-1}\left[K_J(N^{-1}q_m - q_\ell) + D_J(N^{-1}\dot{q}_m - \dot{q}_\ell)\right] \qquad (11b) \end{aligned}$$

the complete dynamic model in Eqn. (10a) and (10b) has extra disturbance terms described by $M_{m\ell}(q_\ell)\ddot{q}_m$, $C_1(q_\ell,\dot{q}_\ell)\dot{q}_m$, and $C_2(q_\ell,\dot{q}_\ell)\dot{q}_\ell$. These disturbances are all related to the motor-link interactive energy described by Eqn. (7).

INFLUENCE EVALUATION OF THE GYROSCOPIC INTERACTION

The difference between the reduced model and the complete dynamic model is caused by the motor-link interactive energy described by Eqn. (7). The influence of the gyroscopic interaction between (the rotors of) the motors and the links can be roughly evaluated by the ratio of the coupled energy term and the link energy term. This ratio can be approximately calculated with only link position and velocity

$$r_s = \frac{2\dot{q}_\ell^T M_{m\ell}(q_\ell) N \dot{q}_\ell}{\dot{q}_\ell^T M_\ell(q_\ell)\dot{q}_\ell} \approx \frac{2\dot{q}_\ell^T M_{m\ell}(q_\ell)\dot{q}_m}{\dot{q}_\ell^T M_\ell(q_\ell)\dot{q}_\ell} \tag{12}$$

which we call the significance ratio.

The upper bound and lower bound of r_s can be evaluated as follows

$$\frac{2\sigma_{\min}(M_{m\ell}(q_\ell)N)}{\sigma_{\max}(M_\ell(q_\ell))} \leq r_s \leq \frac{2\sigma_{\max}(M_{m\ell}(q_\ell)N)}{\sigma_{\min}(M_\ell(q_\ell))}$$

If the upper bound has the property $\sup(r_s) \ll 1$, then the motor-link interaction is negligible, and the system model can be simplified as a reduced model. Otherwise the motor-link interaction can play an important role in the system dynamics, and the complete dynamic model should be used in controller design. A refined threshold can be determined for different cases with specific trajectories. If the requirement of trajectory tracking accuracy is very high, the complete model should be used even for small r_s 's..

EXAMPLE

Two simulators are built using MATLAB SimMechanics. Both have joint flexibility. The first simulator has grounded motors and can be described perfectly using the reduced dynamic model, and the second simulator has a high fidelity representation of motor installation. These two simulators are called the reduced simulator and the complete simulator respectively.

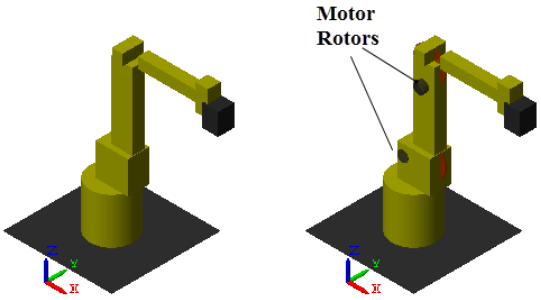

(a) Reduced simulator (b) Complete simulator

FIGURE 1: SIMMECHANICS MODEL OF 6 JOINT INDUSTRIAL ROBOT.

In the simulation, the reference trajectory for the i-th joint is

$$q_{\ell i} = A_i^2 \cos\omega_i t + A_i \sin\omega_i t + \exp(-A_i\omega_i t)$$

where A_i is the amplitude of the steady state sinusoidal motion, ω_i is the angular frequency of the steady state sinusoidal motion. The exponential term is added to guarantee that initial velocity and acceleration are 0. The ω's of all joints are chosen to be smaller than 5 Hz. The reference trajectory in the workspace of the robot is shown in Fig.2.

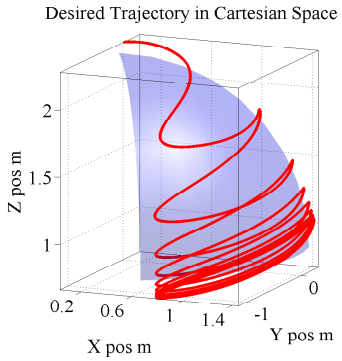

FIGURE 2: REFERENCE TRAJECTORY.

For both simulations, the joint flexibility is handled by adjusting the motor reference using input shaping [10]. The feedforward motor torque is calculated using Eqn. (11b) (the reduced model). A feedback controller $K_p(q_{m\,\text{desire}} - q_m) + K_v(\dot{q}_{m\,\text{desire}} - \dot{q}_m)$ is used for stabilization. The trajectory tracking errors in the workspace of the two simulators are compared in Fig. 3.

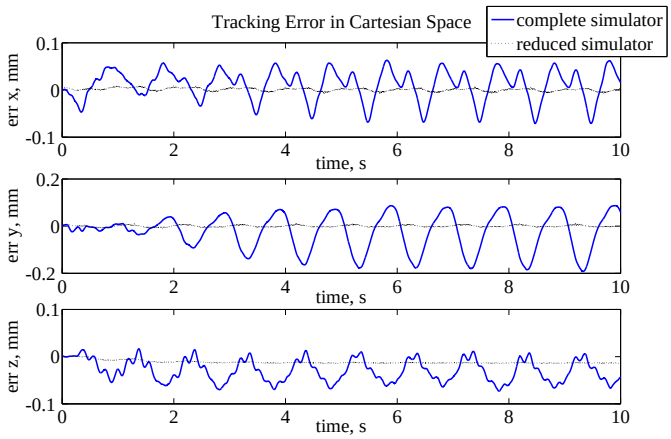

FIGURE 3: COMPARISON OF TRACKING ERRORS.

As shown in Fig. 3, the same motor reference, feedforward torque, and feedback gains are used in the simulations. While

the complete simulator shows significant tracking errors, the reduced simulator fails to predict the errors. This demonstrates the influence of the motor-link gyroscopic interaction.

CONCLUSION

Joint flexibility is common in robots. In this paper, a complete dynamic model for flexible joint robots is derived using Lagrangian dynamics in details. The gyroscopic interactions between the motors and links are fully considered in the resulting model. The significance of the motor-link interaction is evaluated by the ratio of the coupled kinetic energy and the link kinetic energy. It is demonstrated that the trajectory tracking error caused by the gyroscopic interaction can not be ignored for accurate trajectory tracking.

REFERENCES

[1] Litak, G., and Friswell, M. I., 2003. "Vibration in gear systems". *Chaos, Solitons & Fractals,* ***16***(5), pp. 795–800.

[2] Khalil, H. K., and Grizzle, J., 2002. *Nonlinear systems, vol. 3*, Vol. 8. Prentice hall Upper Saddle River.

[3] Hedrick, J., and Yip, P., 2000. "Multiple sliding surface control: theory and application". *Journal of dynamic systems, measurement, and control,* ***122***(4), pp. 586–593.

[4] Yao, B., and Tomizuka, M., 2001. "Adaptive robust control of mimo nonlinear systems in semi-strict feedback forms". *Automatica,* ***37***(9), pp. 1305–1321.

[5] Chen, W., and Tomizuka, M., 2014. "Dual-stage iterative learning control for mimo mismatched system with application to robots with joint elasticity". *Control Systems Technology, IEEE Transactions on,* ***22***(4), pp. 1350–1361.

[6] Spong, M. W., 1987. "Modeling and control of elastic joint robots". *Journal of dynamic systems, measurement, and control,* ***109***(4), pp. 310–318.

[7] De Luca, A., and Book, W., 2008. "Robots with flexible elements". In *Springer Handbook of Robotics*. Springer, pp. 287–319.

[8] Loughlin, C., Albu-Schäffer, A., Haddadin, S., Ott, C., Stemmer, A., Wimböck, T., and Hirzinger, G., 2007. "The dlr lightweight robot: design and control concepts for robots in human environments". *Industrial Robot: an international journal,* ***34***(5), pp. 376–385.

[9] Murray, R. M., Li, Z., Sastry, S. S., and Sastry, S. S., 1994. *A mathematical introduction to robotic manipulation*. CRC press, ch. Rigid Body Motion, pp. 19–80.

[10] Singhose, W., 2009. "Command shaping for flexible systems: A review of the first 50 years". *International Journal of Precision Engineering and Manufacturing,* ***10***(4), pp. 153–168.